THE JOURNAL OF BIOLOGICAL CHEMISTRY VOL. 291, NO. 16, pp. 8465–8474, April 15, 2016

A PWWP Domain of Histone-Lysine *N*-Methyltransferase NSD2 Binds to Dimethylated Lys-36 of Histone H3 and Regulates NSD2 Function at Chromatin*[S]

Received for publication, February 8, 2016, and in revised form, February 23, 2016 Published, JBC Papers in Press, February 24, 2016, DOI 10.1074/jbc.M116.720748

Saumya M. Sankaran[‡], **Alex W. Wilkinson**[‡1], **Joshua E. Elias**[§], **and Or Gozani**[‡2]

From the [‡]*Department of Biology and* [§]*Department of Chemical and Systems Biology, School of Medicine, Stanford University, Stanford, California 94305*

The readout of histone modifications plays a critical role in chromatin-regulated processes. Dimethylation at Lys-36 on histone H3 (H3K36me2) is associated with actively transcribed genes, and global up-regulation of this modification is associated with several cancers. However, the molecular mechanism by which H3K36me2 is sensed and transduced to downstream biological outcomes remains unclear. Here we identify a PWWP domain within the histone lysine methyltransferase and oncoprotein NSD2 that preferentially binds to nucleosomes containing H3K36me2. In cells, the NSD2 PWWP domain interaction with H3K36me2 plays a role in stabilizing NSD2 at chromatin. Furthermore, NSD2's ability to induce global increases in H3K36me2 via its enzymatic activity, and consequently promote cellular proliferation, is compromised by mutations within the PWWP domain that specifically abrogate H3K36me2-recognition. Together, our results identify a pivotal role for NSD2 binding to its catalytic product in regulating its cellular functions, and suggest a model for how this interaction may facilitate epigenetic spreading and propagation of H3K36me2.

Chromatin dynamics play a critical role in the regulation of diverse cellular functions, the dysregulation of which is linked to the development and progression of human diseases. A major mechanism for regulating chromatin functional states involves the reversible covalent post-translational modification of histone proteins by chemical moieties such as methyl-, acetyl-, and phospho- groups. Histones provide a highly modifiable signaling surface on which these chemical marks combine to define particular chromatin states and regulate the extent of accessibility of DNA to trans-acting factors. In this context, the proteins and domains that recognize histone modification fundamentally influence DNA-templated processes, transducing molecular events at chromatin to biological outcomes. Protein lysine methylation is a principal chromatin-regulatory mechanism. The chemical addition of methyl moieties to lysine residues is catalyzed by lysine methyltransferases (KMTs).[3] Lysine residues can accept up to three methyl groups forming mono-, di-, and tri-methylated derivatives (referred to as me1, me2, and me3, respectively). Histone methylation has been linked via methyllysine-binding proteins to diverse processes, including transcription, DNA recombination, DNA repair, and DNA replication.

Methylation of histone H3 at lysine 36 (H3K36) is found at gene bodies of actively transcribed genes, but the state of methylation at this residue defines distinct biological outcomes. Trimethylation of this site (H3K36me3), which is mediated by the KMT SETD2 in humans, is involved in splicing regulation, RNA processing, and DNA damage signaling (1–7). Loss of SETD2 and H3K36me3 is a recurring phenomenon in clear cell renal cell carcinoma (ccRCC) and other cancers, suggesting a tumor suppressor role for SETD2 (8–10). In contrast, the specific molecular functions associated with H3K36me2 are unclear. However, elevated levels of this modification lead to aberrant activation of normally silenced genes (11), and up-regulation of this mark is linked with numerous cancer types including acute myeloid leukemia, multiple myeloma, lung cancers, breast cancers, and glioblastomas (11–14). Thus, different states of methylation at H3K36 (dimethyl *versus* trimethyl) are linked to dramatically different biological and disease-associated readouts.

The bulk of H3K36me2 in a number of cell types is generated by NSD2 (11) a KMT containing a conserved catalytic SET domain and several chromatin-associated domains comprising four PHD fingers, two PWWP domains, and an HMG box. This enzyme is implicated in diverse human diseases. NSD2 haploinsufficiency is associated with the developmental disorder Wolf Hirschhorn syndrome (WHS), which is characterized by growth and mental retardation, congenital heart defects, and antibody deficiencies (15). Indeed, NSD2-deficient mice exhibit a spectrum of defects resembling WHS (16). This enzyme is also implicated in the pathogenesis of the hematologic malignancy multiple myeloma (MM). 15–20% of MM patients carry a translocation between chromosomes 4 and 14 [t(4;14)(p16.3;q32)], which places the transcription of *NSD2* under the control of strong IgH intronic Eμ enhancer and leads to aberrant up-regulation of this gene (17, 18). Furthermore, a recent study in pediatric ALL cell lines and patient samples revealed a recur-

* This work was supported in whole or part by National Institutes of Health Grant R01 GM079641 (to O. G.). O. G. is a co-founder of EpiCypher, Inc. The content is solely the responsibility of the authors and does not necessarily represent the official views of the National Institutes of Health.

[S] This article contains supplemental Tables S1 and S2.

[1] Supported by National Institutes of Health Training Grant T32 GM007276.

[2] To whom correspondence should be addressed: Dept. of Biology, Stanford University, 371 Serra Mall, Stanford, CA. Tel.: 650-736-7639; Fax: 650-725-8309; E-mail: ogozani@stanford.edu.

[3] The abbreviations used are: KMT, lysine methyltransferase; H3K36, histone H3 lysine 36; H3K36me2, dimethylated H3K36; H3K36me3, trimethylated H3K36; MLA, methyl lysine analog; PWWP, Pro-Trp-Trp-Pro conserved motif; EMSA, electrophoretic mobility shift assays.

rent gain-of-function mutation (p.E1099K) in the NSD2 SET domain that confers increased catalytic efficiency of this enzyme, resulting in elevated levels of H3K36me2 (19). These and additional observations support a role for the NSD2 E1099K mutation as an epigenetic-mediated driver in the development of pediatric ALL. This mutation is also found in other cancers (20). Thus, NSD2 plays an important role during mammalian development and its overexpression or hyperactivity may cause cancer.

While dimethylation at H3K36 is associated with oncogenicity, the molecular mechanism underlying this outcome remains unknown. The readout of histone modifications is mediated by effector proteins containing modules that recognize modifications, often with great state- and sequence-specificity. Such "readers" have been identified for H3K36me3, providing direct links to RNA processing (1, 2) and DNA damage (21). However, a reader domain that preferentially binds to the dimethyl state at H3K36 has yet to be identified.

In this study, we performed quantitative proteomic experiments with designer nucleosomes carrying installed methylation at Lys-36. These experiments identified PWWP domains as possible binders of H3K36me2. We directly tested over a dozen PWWP domains for binding to H3K36 methylated nucleosomes. We identified the N-terminal PWWP domains of NSD2 as a preferential binder to H3K36me2. This interaction was found to be important for stable association of NSD2 with chromatin and NSD2 molecular and cellular functions. These results suggest a model in which the ability of NSD2 to bind to the mark it generates plays a role in spreading of H3K36me2 along chromatin as well as epigenetic propagation through cell division.

Experimental Procedures

Protein Sequences and Plasmids—The following full-length and PWWP domain sequences were cloned into pGEX-6p-1 (GE Healthcare) for recombinant protein expression and purification with N-terminal GST fusions: HNRNPA1 (NCBI Accession NP_002127.1), HNRNPAB (NCBI Accession NP_112556.2), TEAD1 (NCBI Accession NP_068780.2), $PSIP1_{PWWP}$ (M1-N64; NCBI Accession NP_001121689.1), $HDGF2_{PWWP}$ (M1-G93; NCBI Accession NP_057157.1), $NSD1_{PWWP1}$ and $NSD1_{PWWP2}$ (S304-D454 and R1696-K1874, respectively; NCBI Accession NP_071900.2), $NSD2_{PWWP1}$ and $NSD2_{PWWP2}$ (P208-E368 and T818-K998, respectively; NCBI Accession NP_001035889.1), $NSD3_{PWWP1}$ and $NSD3_{PWWP2}$ (E247-A402 and S851-A1078, respectively; NCBI Accession NP_075447.1), $MSH6_{PWWP}$ (D89-E192; NCBI Accession NP_000170.1), $DNMT3A_{PWWP}$ (G278-E427;NCBI Accession NP_072046.2), $DNMT3B_{PWWP}$ (E206-P355; NCBI Accession NP_008823.1), $MBD5_{PWWP}$ (S1371-R1494; NCBI Accession NP_060798.2), $MUM1L1_{PWWP}$ (W406-K539; NCBI Accession NP_001164491.1), $N\text{-}PAC_{PWWP}$ (M1-S114; NCBI Accession NP_115958.2). Full-length NSD2 was cloned into Gateway pENTR 3C vector (Life Technologies), then recombined into mammalian expression vector pLenti6.2/V5-DEST (Life Technologies) or into pMSCVpuro (Clontech) modified with an N-terminal FLAG-myc affinity tag and a destination cassette (Life Technologies). Single point mutations were introduced into the NSD2 sequence by site-directed mutagenesis.

Cell Culture and Transfections—HeLa, HEK 293T, and HT1080 cells were cultured in DMEM (Life Technologies) supplemented with 10% fetal bovine serum (Gibco/Life Technologies), penicillin-streptomycin (Life Technologies), L-glutamine (Life Technologies), sodium pyruvate (Life Technologies), and MEM non-essential amino acids (Life Technologies). Viral transductions were performed as previously described (11) to generate HT1080 cells stably expressing NSD2 WT or derivative mutants. Cells transduced with pMSCVpuro-FLAG-myc-NSD2 were selected under puromycin (Sigma) at 2 μg/ml, and those with pLenti6.2/v5-DEST-NSD2 were selected under blasticidin (Life Technologies) at 10 μg/ml.

Antibodies—The antibodies used were: GST (generated at Covance), histone H3 (EpiCypher), NSD2 (EpiCypher), β-tubulin (Millipore, catalogue no. 05-661), H3K36me1 (Cell Signaling Technology, catalogue no. 14111S), H3K36me2 (Cell Signaling Technology, catalogue no. 2901S), H3K36me3 Cell Signaling Technology, catalogue no. 4909S), and FLAG M2 (Sigma, catalogue no. F1804). Antibodies against methylated H3K36 were validated by probing a custom peptide array as previously described (22).

Peptides, MLA Histones, and Recombinant Nucleosomes—Histone H3(21–44) N-terminally biotinylated peptides were synthesized with unmodified, mono-, di-, or tri-methylated lysine at Lys-36 (ATKAARKSAPATGGVK_{me}KPHRYRPG) at the Stanford Protein and Nucleic Acid facility. Recombinant *Xenopus laevis* core histones were expressed, purified, and assembled into mononucleosomes with 5′ biotinylated 186 bp "Widom" 601 sequence DNA as previously described (23). To generate methylated full-length histones, single lysine-to-cysteine point mutations (K4C, K9C, K27C, K36C, K79C) were incorporated into the H3 sequence by site-directed mutagenesis. These H3 mutant constructs were recombinantly expressed, and mono-, di-, or tri-methyl modifications were installed on the introducted cysteine residues using MLA chemistry, as previously described (24). Modified histones were verified by LC-ESI/MS with a MicrO-TOF-QII (Bruker) mass spectrometer.

SILAC Protein Pulldowns and Quantitative Mass Spectrometry—HeLa cells grown in SILAC media with light amino acids (L-lysine/L-arginine, AppliChem) or heavy amino acids (L-[$^{13}C^{15}N$]lysine/L-[$^{13}C^{15}N$]arginine Thermo Scientific) were used to prepare nuclear extracts as described (25, 26). Nucleosome pulldowns indicated in Fig. 1*A* were performed as previously described (27) using 5 μg of the recombinant nucleosomes described above, 100 μl Dynabeads MyOne Streptavidin T1 (Thermo Fisher Scientific) slurry, and 500 μg nuclear extract per pulldown. Precipitated proteins were separated by SDS-PAGE, subjected to in-gel digest with trypsin (Promega) as previously described (26), and analyzed by LC-MS/MS on an Orbitrap Elite mass spectrometer. Raw mass spectra were analyzed using MaxQuant version 1.3.0.5 (28).

Recombinant Protein Preparation and Pulldown Assays—GST-fusion proteins were expressed in BL21 *Escherichia coli* with 0.1 mM IPTG (Sigma), purified using glutathione-Sepharose 4B (GE Healthcare) beads, and eluted with reduced L-glu-

tathione (Sigma). Protein concentrations were measured using the Coomassie Plus assay (Pierce). For direct pulldown assays, 1 μg of biotinylated peptide or 5 μg of biotinylated recombinant nucleosome was immobilized on 20-μl Streptavidin Sepharose High Performance beads (GE Healthcare), incubated with 5 μg of recombinant protein in binding buffer (50 mM Tris-HCl, pH 7.5, 150 mM NaCl, 0.05% (*v*/*v*) Nonidet P-40, 1 mM PMSF) overnight at 4 °C, and washed three times in buffer before analysis by Western blot.

Electromobility Shift Assays—Nucleosomes were incubated with recombinant GST-PWWP domains in EMSA buffer (20 mM Tris, pH 8.0, 1 mM EDTA, 1 mM DTT, 10% glycerol) for 30 min at room temperature and analyzed by native 0.2× TBE PAGE. Each reaction contained 1 pmol of nucleosome with the indicated pmol of domain. Gels were stained with ethidium bromide, and bands were analyzed using an in-house iPython script. Intensity of NCP band was measured, and loss of free NCP was used to calculate fraction of NCP bound.

Cell Fractionation and Lysates—Biochemical fractionation was adapted from a protocol previously described (29). Briefly, 1×10^7 cells per cell line were collected, washed in PBS, and lysed in Buffer A (10 mM HEPES pH 7.9, 10 mM KCl, 1.5 mM $MgCl_2$, 0.34 M sucrose, 10%glycerol, 1 mM DTT, Complete protease inhibitor tablet (Roche)), containing Triton X-100 at a final concentration of 0.1%, for 10 min on ice. Cytoplasmic proteins were separated from nuclei by centrifugation at 1300 × *g* for 5 min at 4 °C. Nuclei pellets were washed in Buffer A and lysed in Buffer B (3 mM EDTA, 0.2 mM EGTA, 1 mM DTT, Complete protease inhibitor) for 30 min on ice, and soluble proteins were separated from chromatin by centrifugation at 1700 × *g* for 5 min at 4 °C. Nuclear proteins were extracted by incubating nuclei pellets in Buffer B with 150 mM NaCl for 20 min on ice, followed by centrifugation at 1700 × *g* for 5 min at 4 °C, and the supernatant was collected as the 150 mM salt soluble nuclear fraction. The remaining nuclei pellets were incubated in Buffer B with 300 mM NaCl for 20 min on ice, followed by centrifugation at 1700 × *g* for 5 min at 4 °C, and the resulting supernatant was collected as the 300 mM salt soluble nuclear fraction. Chromatin pellets were resuspended in the SDS sample buffer and solubilized by sonication for 10 min in a Bioruptor (Diagenode).

For whole cell extracts, 1×10^7 cells per cell line were collected, washed in PBS, and lysed in a RIPA buffer (50 mM Tris-HCl, pH 7.4, 150 mM NaCl, 2 mM EDTA, 1% Nonidet P-40, 0.1% SDS, 1 mM DTT, Complete protease inhibitor tablet (Roche)) for 10 min on ice followed by sonication for 10 min in a Bioruptor. Samples were clarified by centrifugation at 21,000 × *g* for 10 min at 4 °C. For normalization, protein concentrations were measured using the DC Protein Assay kit (Bio-Rad).

Chromatin Immunoprecipitation and Quantitative PCR—ChIP and quantitative real-time PCR were performed as previously described (11). The primer sequences used in this study were: CDC42 primer 1 (promoter) forward, 5′-ATGTTCCCC-ATCTGGTGCT-3′; CDC42 primer 1 (promoter) reverse, 5′-GGCAACTTTCAAAAAGGAGTATGT-3′; CDC42 primer 2 (TSS-proximal region) forward, 5′-CAACTGTGCGTCTCCT-GCGCG-3′; CDC42 primer 2 (TSS-proximal region) reverse, 5′-GGCAGCACTGCGCGGGGTCTC-3′; CDC42 primer 3 (3′ exon) forward, 5′-GGCAGGTGGATCACTTACTTG-3′; CDC42 primer 3 (3′ exon) reverse, 5′-TTTTAGCAGACACG-GGGTTT-3′; MYC (TSS-proximal region) forward, 5′-AGG-GATCGCGCTGAGTATAA-3′; MYC (TSS-proximal region) reverse, 5′-TGCCTCTCgCTGGAATTACT-3′; TGFA (TSS-proximal region) forward, 5′-GTTGAAAGCGACGAAAC-CAT-3′; and TGFA (TSS-proximal region) reverse, 5′-GTT-GAAAGCGACGAAACCAT-3′.

Results

Proteomic Screen for Candidate H3K36 Methyl-binding Proteins using Modified Nucleosome Substrates—Reader domains of histone tail PTMs are often identified using peptides chemically synthesized with the modified residue of interest. However, based on the proximity of the histone H3 Lys-36 residue to the nucleosome core, recognition of H3K36 modifications by reader domains may be influenced by structural components of the core. Indeed, the majority of H3K36me3 reader domains show stronger binding to substrates comprising both the histone modification and DNA (such as nucleosomes) than to the modification alone (30). We therefore reasoned that any potential H3K36me2-specific binding domain would likely also require reading the modification in a nucleosomal context. To test this hypothesis, we assembled recombinant nucleosomes (23) with histones modified by methyl lysine analog (MLA) chemistry (24) to install the different states of methylation at H3K36 ($H3K_CK36me1$, $H3K_C36me2$, and $H3K_C36me3$). The nucleosome DNA was 5′-biotinylated to allow for high-affinity purification of these designer nucleosomes, which coupled with SILAC (*S*table *I*sotope *L*abelling by *A*mino acids in *C*ell culture)-based quantitative proteomic screening can be used to search in an unbiased manner for proteins that preferentially bind to H3K36me2 (27).

We used this system to isolate proteins from nuclear extracts that bound differentially to $H3K_C36me2$ or $H3K_C36me3$ *versus* H3K36 unmodified nucleosomes (see experimental outline in Fig. 1*A*). This analysis identified enrichment of several proteins binding to $H3K_C36me2$ nucleosomes (Fig. 1*B*). We note that the majority of these hits were also found in the $H3K_C36me3$ pulldowns (Fig. 1*B* and supplemental Tables S1 and S2), and included proteins containing a PWWP domain, a known H3K36me3-binding module (30–32), several proteins in the HNRNP family, RAN-associated proteins, and a few other proteins that did not segregate into a particular group. We tested the top hits for direct binding to $H3K_C36me2/3$ nucleosomes. The HNRNP family proteins HNRNPA1 and HNRNPAB, bound nonspecifically to substrates regardless of methyl state, while the transcriptional activator TEAD1 showed no binding to any of the substrates (Fig. 1*C*). In contrast, we found that two PWWP-containing proteins, PSIP1/LEDGF and HDGF2, bound to H3K36 methylated nucleosomes (see Fig. 2*B*). PSIP1 has previously been characterized to bind H3K36me3-containing nucleosomes, though its ability to bind to other states of methylation at H3K36 has not previously been tested (32).

Analysis of Human PWWP Domains Binding to H3K36 MLA-modified Nucleosomes—As previous studies of PSIP1 and other PWWP domains binding to H3K36me3-containing nucleosomes did not test H3K36me2-containing nucleosomes

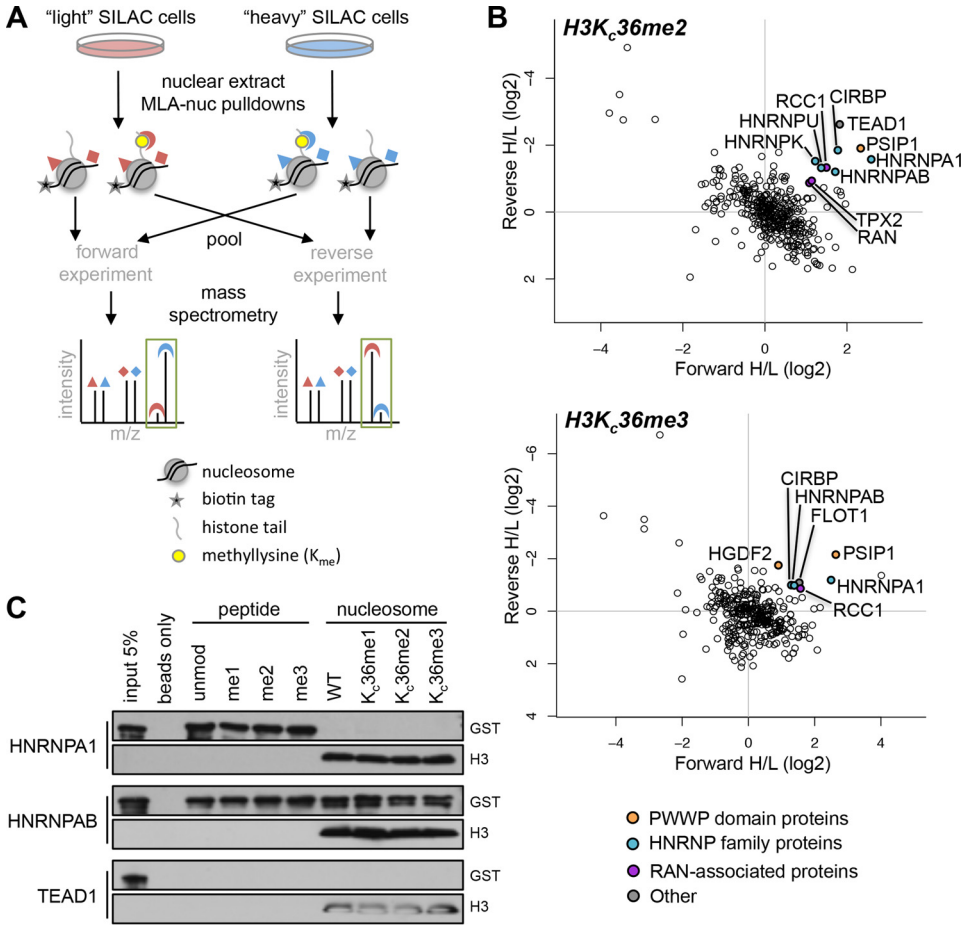

FIGURE 1. **Proteome-wide screen for H3K36 methyl binding proteins using modified nucleosome substrates.** *A*, schematic of proteomic approach to screen for candidate H3K36 methyl binders from SILAC nuclear extract. *B*, enrichment of proteins bound to MLA H3K$_C$36me2 (*top*) or H3K$_C$36me3 (*bottom*) nucleosomes over unmodified nucleosome substrates. Identified proteins are plotted by SILAC ratio in the forward (*x* axis) and reverse (*y* axis) experiments, with candidate H3K36 methyl binders in the *top right quadrant*. Proteins enriched with ratio >1.8 (log2 ratio > 0.85) in the forward SILAC experiment and <0.55 (log2 ratio < −0.85) in the reverse SILAC experiment are labeled and categorized as PWWP domain proteins (*orange*), HNRNP family (*cyan*), RAN-associated (*magenta*), or Other (*gray*). *C*, Western blot analysis of direct pulldown assays testing binding of the indicated GST fusion proteins to H3 tail (21–44 aa) peptide substrates bearing umodified (unmod), monomethyl (me1), dimethyl (me2), or trimethyl (me3) H3K36, or the indicated MLA H3K$_C$36 nucleosomes.

as a potential substrate, we undertook a candidate approach and screened the majority of human PWWP domains for preferential binding to H3K36me2 (Fig. 2*A*). We performed binding assays using recombinant PWWP domains and mono-, di-, or tri- methylated H3K36 substrates in the form of biotinylated H3 tail peptides (amino acids 21–44) or the MLA nucleosomes (Fig. 2, *B–D*). As shown in Fig. 2*B*, PWWP domains from the proteins PSIP1, DNMT3A, and DNMT3B bound preferentially to H3K36me3, consistent with the binding activity previously reported for these domains (Fig. 2*B*) (32–34). Our screen also identified HDGF2$_{PWWP}$ as an H3K36me3-binding module, consistent with its high degree of conservation with PSIP1 (Fig. 2*B*). The MSH6$_{PWWP}$, which was also reported to bind H3K36me3 (21), bound in our assay to nucleosomes irrespective of the state of methylation at Lys-36; however we note that binding to H3K36me3 peptide was stronger than the other peptides (Fig. 2*B*).

Notably, our screen revealed two PWWP domains, an N-terminal PWWP of NSD2 (NSD2$_{PWWP1}$) and a similar PWWP domain within NSD3 (NSD3$_{PWWP1}$), which bound preferentially to H3K36me2 *versus* the other K36 methyl states and did so in a nucleosomal context but not on peptides (Fig. 2*C*). In contrast, the first PWWP of NSD1 did not show the same specific binding as the other two NSD family members. An alignment of these three PWWP domains shows that the sequence flanking the canonical PWWP motif comprises aromatic and aliphatic residues that are conserved between NSD2 and NSD3 but contains basic residues in these positions on NSD1 (Fig. 2*A*), which could significantly alter binding affinity for histone substrates. Like the first PWWP of NSD1, no binding or no methyl-specific binding was observed for the second PWWP domains found on NSD1, NSD2 and NSD3 (NSD1$_{PWWP1}$, NSD2$_{PWWP2}$ and NSD3$_{PWWP2}$, respectively), or the PWWP domains from MBD5, MUM1L1, and N-PAC (Fig. 2*D*). Together, our results identify PWWP domains found within NSD2 and NSD3, two H3K36 lysine di-methltransferases (11, 35), as potential H3K36me2-binding modules. Here we focus our studies on the NSD2$_{PWWP1}$ as NSD2 plays a clear role in the etiology of several cancers and is important for regulating the bulk of H3K36me2 in multiple cell types(11).

N-terminal PWWP Domain of NSD2 Preferentially Binds H3K36me2-modified Nucleosomes—Besides H3K36, histone H3 in humans bears four additional canonical lysine methylation sites: H3K4, H3K9, H3K27, and H3K79. We next tested the

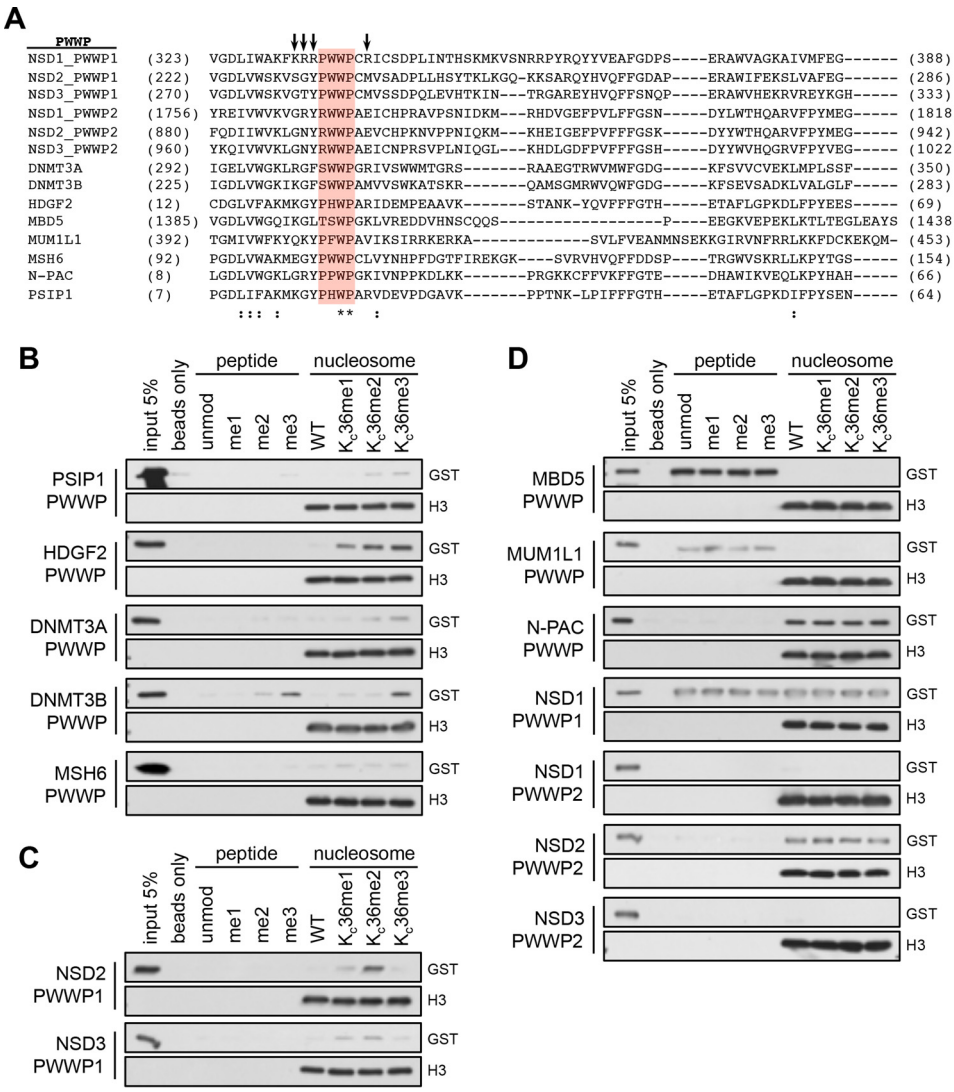

FIGURE 2. **Candidate screen of human PWWP domains reveals $NSD2_{PWWP1}$ and $NSD3_{PWWP1}$ as H3K36 methyl readers.** *A,* sequence alignment of selected human PWWP domains. The PWWP motif is highlighted. *Arrows* indicate residues that are similar between NSD2 and NSD3 but not NSD1. *, conserved residue. :, similar residues. *B–D,* Western blot analysis of pulldown assays testing direct binding of the indicated PWWP domains as in Fig. *1C*. H3K36me3-binding domains are grouped in *B*, domains with preferential binding to H3K36me2 are shown in *C*, and the non-binding or nonspecific binding domains are grouped in *D*.

sequence specificity of $NSD2_{PWWP1}$ in binding assays using MLA nucleosomes dimethylated at each of the five canonical lysines on H3. As shown in Fig. 3*A*, $NSD2_{PWWP1}$ bound to $H3K_C36me2$ but did not bind to the other dimethyl lysine sites. Based on these data we conclude that $NSD2_{PWWP1}$ shows high specificity for H3K36me2, making this domain to our knowledge the first known reader to have specificity for H3K36me2.

To assess the binding specificity of $NSD2_{PWWP1}$ for $H3K_C36me2$ *versus* $H3K_C36me3$ nucleosomes by an independent and more quantitative method, we characterized the PWWP-nucleosome interaction in electrophoretic mobility shift assays (EMSA) (Fig. 3*B*). The apparent K_d of the $NSD2_{PWWP1}$-$H3K_c36me2$ interaction was ~0.25 μM *versus* ~0.57 μM for $H3K_c36me3$ nucleosomes (Fig. 3, *C* and *D*). As a control, we also analyzed binding of the known H3K36me3 reader $PSIP1_{PWWP}$, which bound to $H3K_C36me3$ nucleosomes with an apparent K_d of ~0.67 μM, similar to previous reports (32) and at ~0.93 μM for $H3K_C36me2$ (Fig. 3*D*, data not shown). Taken together, we conclude that $NSD2_{PWWP1}$ is a reader domain of methylated H3K36, with preference for the dimethyl state.

The PWWP-H3K36me2 Interaction Stabilizes NSD2 at Chromatin—To explore the functional implications of the $NSD2_{PWWP1}$-H3K36me2 interaction, we first sought to identify point mutations within the PWWP domain that would specifically abrogate binding. Essential for all known methyllysine-binding domains is the presence of a hydrophobic, aromatic cage to encapsulate the modified residue (36). To identify residues within $NSD2_{PWWP1}$ that potentially form the aromatic cage and mediate H3K36me2-recognition, we aligned the sequence of this domain with that of $PSIP1_{PWWP}$, for which a structure has been solved (32, 37) (Fig. 4*A*). This analysis identified Trp-236 and Phe-266 on NSD2 as conserved aromatic residues that could form the H3K36 methyllysine-binding pocket. We found that substitution of either of these residues to an alanine abrogated

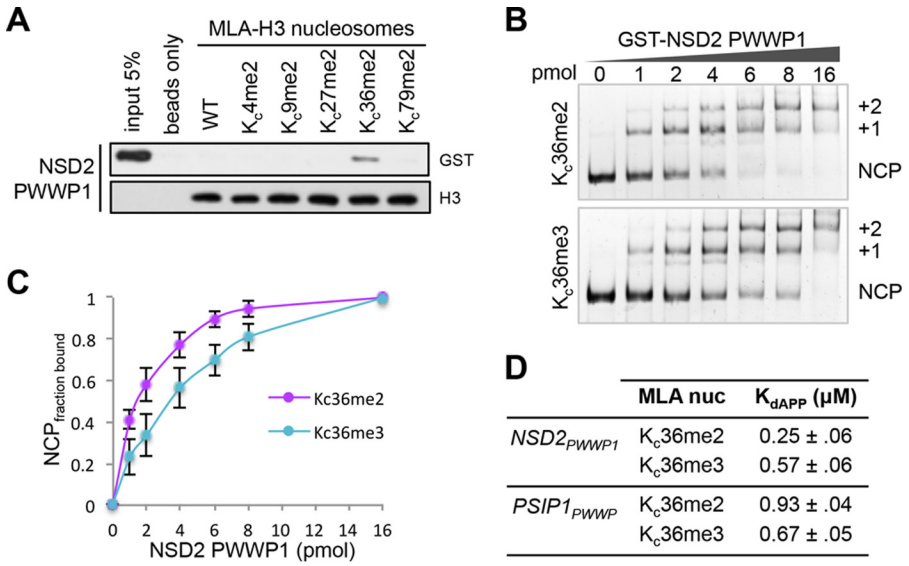

	MLA nuc	K_{dAPP} (μM)
$NSD2_{PWWP1}$	K_c36me2	0.25 ± .06
	K_c36me3	0.57 ± .06
$PSIP1_{PWWP}$	K_c36me2	0.93 ± .04
	K_c36me3	0.67 ± .05

FIGURE 3. **$NSD2_{PWWP1}$ preferentially binds H3K36me2-modified nucleosomes.** *A*, Western blot analysis as in Fig. *2B* of GST-$NSD2_{PWWP1}$ binding to nucleosomes carrying dimethyl analogs at the indicated H3 lysine residues. *B*, titration of GST-$NSD2_{PWWP1}$ against MLA H3K_C36me2 (*top*) or H3K_C36me3 (*bottom*) nucleosomes in EMSA. Bands indicated correspond to free nucleosome core particle (*NCP*) and nucleosome bound by one (+1) or two (+2) PWWP molecules. *C*, binding curves quantified from EMSA experiments of GST-$NSD2_{PWWP1}$ on MLA H3K_C36me2 or H3K_C36me3 nucleosomes. Error bars represent S.E. from three independent experiments. *D*, apparent binding affinity (K_{dAPP}) for H3K_C36me2 and H3K_C36me3 nucleosomes calculated from binding curves for GST-$NSD2_{PWWP1}$ in *C* and for GST-$PSIP1_{PWWP}$ (data not shown). Error indicates S.E. from three independent experiments.

$NSD2_{PWWP1}$ binding to H3K36me2 in direct nucleosome pulldown assays (Fig. 4*B*).

We next investigated the role of H3K36me2-binding by $NSD2_{PWWP1}$ on the function of this enzyme in cells. As the major H3K36 dimethyltransferase in many cell types, NSD2 is generally tightly bound at chromatin (11). We therefore postulated that the $NSD2_{PWWP1}$-H3K36me2 interaction might regulate NSD2 stability at chromatin. To test this idea, we established HT1080 cell lines stably expressing either full-length wild-type Flag-myc-NSD2 or the F266A mutant derivative. Lysates from these cells were used for biochemical fractionation to assess chromatin association using a modified Stillman fractionation protocol (see schematic in Fig. 4*C*; Ref. 29). As shown in Fig. 4*D*, the wild-type protein remained largely bound to chromatin through 300 mM salt washes, whereas the mutant protein showed weaker chromatin association, with a more equal distribution between the high salt soluble nuclear fraction and the chromatin fraction. These data are consistent with a role for the $NSD2_{PWWP1}$-H3K36me2 interaction in stabilizing NSD2 at chromatin.

We next tested whether the ability of NSD2 to recognize H3K36me2 via its PWWP domain impacts target gene occupancy. Chromatin immunoprecipitation (ChIP) assays with anti-Flag coupled with quantitative PCR was used to assess binding of Flag-myc-NSD2 wild-type or F266A at the *CDC42* gene, an NSD2 target identified by ENCODE (38–40). Enrichment of NSD2 signal was far greater at the promoter, TSS-proximal region, and 3′-end terminus of *CDC42* gene (Fig. 4*E*, *top panel*) in cells expressing wild-type NSD2 compared with the F266A mutant derivative or the vector alone (Fig. 4*E*, *middle panel*). Occupancy of the NSD2 H3K36me2-binding mutant was only slightly higher than the vector control (Fig. 4*E*, *middle panel*) and largely similar to the signal seen with the IgG control ChIP from the three cell lines (Fig. 4*E*, *bottom panel*). Similar trends were observed at TSS-proximal regions of two additional NSD2 target genes, MYC and TGFA (11) (Fig. 4, *F* and *G*, respectively). Together, these data support a role for the interaction between the first PWWP domain of NSD2 and H3K36me2 in stabilizing NSD2 at chromatin and regulating NSD2 occupancy at its gene targets.

Regulation of NSD2 Cellular Functions by the PWWP-H3K36me2 Interaction—The major molecular function of NSD2 is to generate the bulk of H3K36me2 in cells, and overexpression of NSD2 alone is sufficient to elicit changes in the global levels of H3K36me2 (11). To test if PWWP-recognition of H3K36me2 impacted this NSD2 activity, we compared global levels of H3K36me2 in HT1080 cells moderately overexpressing NSD2 WT, two different PWWP1 mutants that abrogate H3K36me2-binding, a catalytically dead mutant (NSD2 Y1092A, a previously characterized catalytically dead mutant referred to here as $NSD2_{CDM}$ (11), or the vector alone as a control (Fig. 5*A*). As expected, NSD2 expression specifically increased H3K36me2 levels relative to control and $NSD2_{CDM}$ (Fig. 5*A*). Expression of the two PWWP mutants, NSD2 W236A and NSD2 F266A, also resulted in a global increase in H3K36me2 levels relative to control and $NSD2_{CDM}$ but were impaired in this activity relative to wild-type NSD2 (Fig. 5*A*). No changes in H3K36me1 or H3K36me3 levels were observed, in keeping with previous studies of NSD2 regulating H3K36 dimethylation (11). Together, these results suggest that the PWWP domain does not directly impact NSD2 catalytic activity, but the ability to bind to H3K36me2 nonetheless regulates generation of this modification in cells by a non-catalytic mechanism.

Overexpression of NSD2, in addition to causing a global increase in H3K36me2 levels, is also known to increase cellular proliferation rates (11, 39). To test the role of H3K36me2-recognition in this function, we established HT1080 cell lines stably expressing NSD2 and various mutants. As shown in Fig. 5*B*,

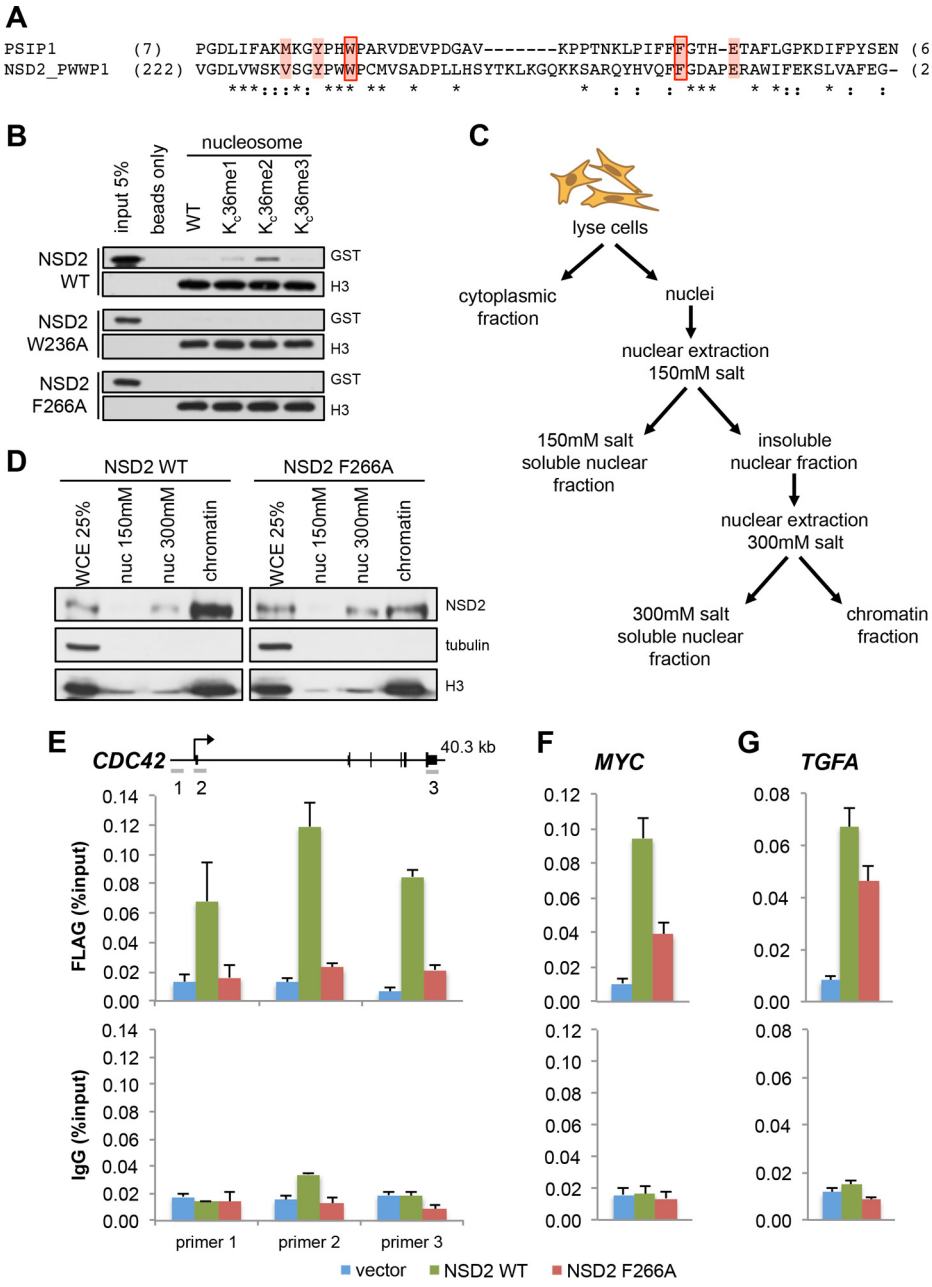

FIGURE 4. **PWWP-H3K36me2 binding stabilizes NSD2 chromatin association.** *A*, sequence alignment of $PSIP1_{PWWP}$ and $NSD2_{PWWP1}$. Residues involved in the $PSIP1_{PWWP}$ H3K36me3-binding aromatic cage are highlighted. *Boxes* indicate residues chosen for mutational analysis. *B*, mutation of the indicated aromatic cage residues abrogates $NSD2_{PWWP1}$ binding to $H3K_C36me2$ in direct pulldown assays as in Figs. *1C* and *2*, *B–D*. *C*, schematic of modified Stillman fractionation method to biochemically separate chromatin-associated proteins from soluble nuclear proteins in cellular extracts. *D*, Western blot analysis of biochemical fractions defined in *C* from HT1080 cells expressing full-length FLAG-myc-NSD2 wild-type or F266A PWWP1 mutant shows altered chromatin association for the PWWP1 mutant derivative. Tubulin and H3 blots serve as controls for intact fractions. *WCE*, whole cell extract. *nuc 150*, 150 mM salt soluble nuclear fraction. *nuc 300*, 300 mM salt soluble nuclear fraction. *chromatin*, chromatin fraction. *E*, ChIP analysis of FLAG-myc-NSD2 wild-type or F266A occupancy across *CDC42* gene. A schematic of the gene (*top panel*) indicates the location of primers used for qPCR analysis of FLAG (*middle panel*) or IgG control (*bottom panel*) ChIP from each stable cell line. vector, HT1080 cells transduced with empty vector. Error bars indicate S.E. from three experiments. *F* and *G*, ChIP analysis as in *E* at TSS-proximal sites (analogous to *CDC42* primer 2) of NSD2 gene targets MYC and TGFA, respectively.

cells expressing wild-type NSD2 grew faster than the vector control-treated cells. In contrast, cells expressing NSD2 derivatives harboring mutations in the PWWP domain that abrogate H3K36me2-binding did not increase the proliferation rate of the cells, displaying growth that was comparable to cells expressing the vector control and the catalytic dead mutant (Fig. 5, *B* and *C*). Taken together, these data demonstrate that the ability of the NSD2 N-terminal PWWP domain to bind to H3K36me2 is important for NSD2's ability to, upon overexpression, generate H3K36me2 and promote cellular proliferation, two activities that are linked to the oncogenic potential of this epigenetic factor.

Discussion

Here we report the N-terminal PWWP domain of the lysine methyltransferase NSD2 as a reader of H3K36me2. While other

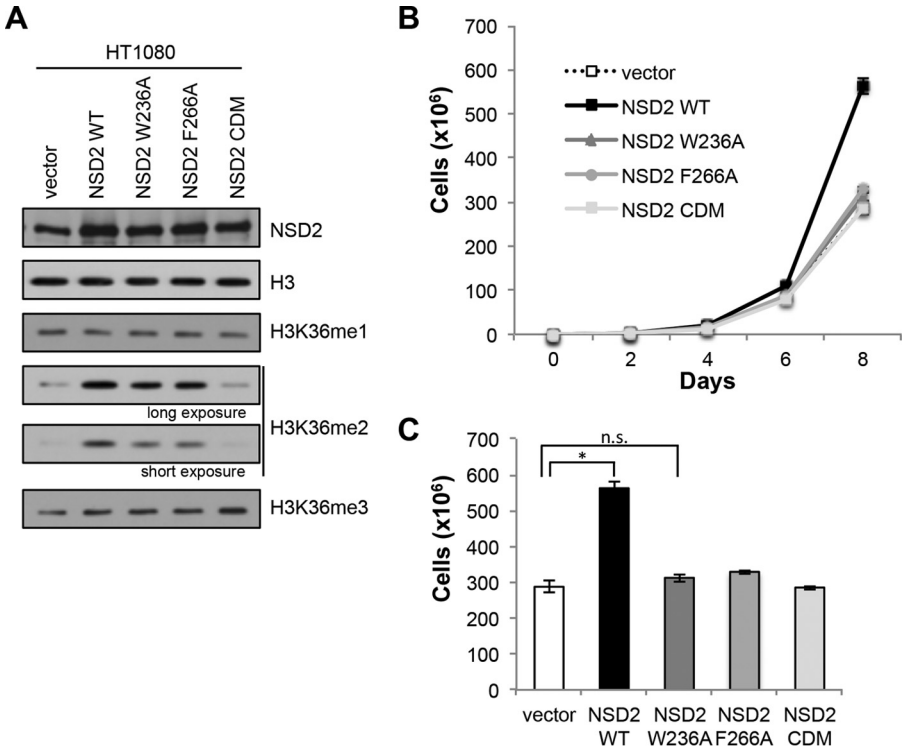

FIGURE 5. **PWWP-H3K36me2 interaction regulates NSD2 cellular functions.** *A*, Western blot analysis with the indicated antibodies on lysates from HT1080 cells expressing NSD2 wild-type or mutant derivatives. vector, HT1080 cells transduced with empty vector. *CDM*, catalytic dead mutant. *B*, proliferation assays using the cells described in *A* counted over 8 days. Error bars indicate S.E. from three experiments. *C*, cell counts from Day 8 of the proliferation assay in *B*. *p* values were calculated using a two-tailed Student's *t* test. *, $p < 0.01$. *n.s.*, not significant.

PWWP domains have been reported as H3K36me3 readers, this is the first instance of a methyllysine binding domain showing preference for the dimethyl state of H3K36 over the trimethyl state (Fig. 3, *C* and *D*). Our data further show that this interaction is not detectable on histone tail peptides alone, but occurs robustly and specifically in the physiologically relevant context of a nucleosome substrate (Figs. 2*C* and 3*A*).

Interestingly, the modification recognized by the NSD2 PWWP domain is the same one deposited by NSD2's catalytic SET domain. We propose that the $NSD2_{PWWP1}$ and $NSD2_{SET}$ domains cooperate to recognize nucleosomes carrying H3K36me2 and deposit the same modification on neighboring nucleosomes (Fig. 6*A*). Such a mechanism could lead to NSD2-mediated spreading of H3K36me2 across nucleosomes (Fig. 6*B*, *top*) to generate regions of H3K36me2 occupancy. Propagation of a modification may also function in maintenance after DNA replication (Fig. 6*B*, *bottom*), whereby the original H3K36me2-bearing nucleosomes that get distributed into the two daughter DNA strands serve as a template to fill in the modification on newly incorporated histones, thus reestablishing the regions of H3K36me2 occupancy in the daughter cells. Indeed, our results show that cells overexpressing NSD2 PWWP mutants do not generate as much global H3K36me2 as cells overexpressing wild-type NSD2 (Fig. 5*A*). These data are consistent with a role for the PWWP-H3K36me2 interaction in propagating this modification.

The presence of modules that both recognize and "write" the same histone modification within a single protein or complex has previously been linked to propagation of two silencing histone modifications. Such a mechanism was first described for H3K9me3 (41–43), and later for H3K27me3 (44). In contrast, our study presents the first instance of such a connection between methyl reader and writer modules for a histone modification associated with actively transcribed genes, H3K36me2.

NSD2 has been characterized as a powerful driver of multiple myeloma and general oncogenic programming (11, 45). Specifically, this oncogenic potential is dependent on NSD2's catalytic function and consequent up-regulation of global H3K36me2 levels (11). This in turn mediates global activation of gene transcription and leads to aberrant cell growth through mechanisms yet to be elucidated. In our study, we note that overexpression of NSD2 PWWP mutants (whose catalytic domains are unaltered) does not lead to increased cell proliferation as does overexpressed wild-type NSD2. This suggests that the NSD2 PWWP-mediated propagation of H3K36me2 may be important in directing this modification to target loci, or creating regions of increased local concentration of H3K36me2, to transduce a downstream biological outcome. Elucidating the specific role of the PWWP-H3K36me2 interaction in stabilizing NSD2 at chromatin will be important in further understanding the function of NSD2 and the H3K36me2 modification in normal physiologic conditions as well as aberrant disease states. Furthermore, given the difficulty in generating inhibitors of the catalytic activity of NSD2, our results suggest an alternative strategy of blocking the PWWP-H3K36me2 interaction with small molecule inhibitors that may lead to therapeutic options for NSD2-driven cancers.

Taken together, our data identify the N-terminal PWWP domain of NSD2 as the reader domain that preferentially binds

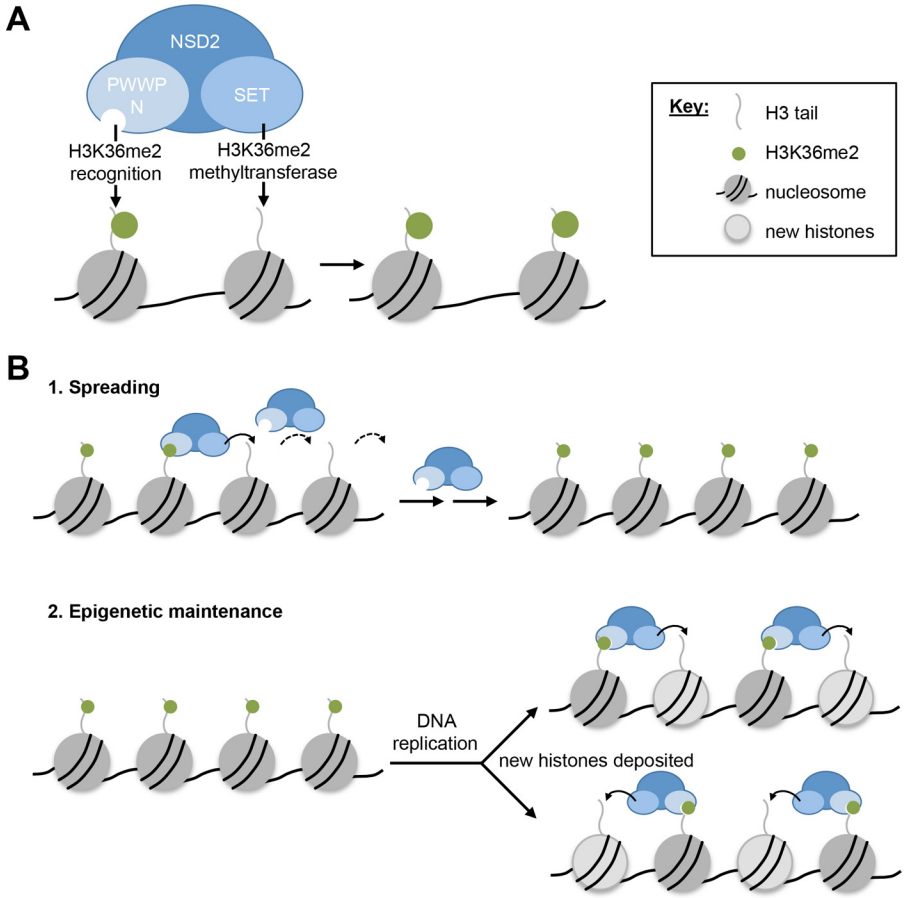

FIGURE 6. **A model for propagation of H3K36me2 by NSD2.** *A*, the N-terminal PWWP domain and SET domain of NSD2 cooperate to recognize nucleosomes carrying H3K36me2 and deposit the same mark on neighboring nucleosomes, thus propagating this modification. *B*, by this mechanism of propagation, NSD2 mediates the spreading of H3K36me2 across a genomic region (*top*) or maintenance of H3K36me2 patterns in daughter cells after DNA replication, when parental histones have been distributed between daughter cells and new histones have been incorporated (*bottom*).

to H3K36me2. We provide evidence that this molecular interaction is important for NSD2-driven up-regulation of H3K36me2 levels and increased cell proliferation, both of which are implicated in this enzyme's oncogenic potential.

Author Contributions—S. M. S. performed the experiments and analyzed data. A. W. W. constructed the bacterial expression constructs, generated MLA histones, and provided technical assistance. O. G. supervised the work, J. E. E. supervised mass spectrometry, and S. M. S. and O. G. designed experiments and wrote the paper. All authors reviewed the results and approved the final version of the manuscript.

References

1. Guo, R., Zheng, L., Park, J. W., Lv, R., Chen, H., Jiao, F., Xu, W., Mu, S., Wen, H., Qiu, J., Wang, Z., Yang, P., Wu, F., Hui, J., Fu, X., Shi, X., Shi, Y. G., Xing, Y., Lan, F., and Shi, Y. (2014) BS69/ZMYND11 reads and connects histone H3.3 lysine 36 trimethylation-decorated chromatin to regulated pre-mRNA processing. *Mol. Cell* **56,** 298–310
2. Wen, H., Li, Y., Xi, Y., Jiang, S., Stratton, S., Peng, D., Tanaka, K., Ren, Y., Xia, Z., Wu, J., Li, B., Barton, M. C., Li, W., Li, H., and Shi, X. (2014) ZMYND11 binds K36me3 and regulates PolII elongation. *Nature* **508,** 263–268
3. Luco, R. F., Pan, Q., Tominaga, K., Blencowe, B. J., Pereira-Smith, O. M., and Misteli, T. (2010) Regulation of alternative splicing by histone modifications. *Science* **327,** 996–1000
4. Spies, N., Nielsen, C. B., Padgett, R. A., and Burge, C. B. (2009) Biased chromatin signatures around polyadenylation sites and exons. *Mol. Cell* **36,** 245–254
5. Jha, D. K., and Strahl, B. D. (2014) PolII-Set2 in DSB repair activation. *Nat. Commun.* **5,** 1–12
6. Pai, C.-C., Deegan, R. S., Subramanian, L., Gal, C., Sarkar, S., Blaikley, E. J., Walker, C., Hulme, L., Bernhard, E., Codlin, S., Bähler, J., Allshire, R., Whitehall, S., and Humphrey, T. C. (2014) H3K36 switch in DNA DSB repair pathway choice. *Nat. Commun.* **5,** 1–11
7. Jha, D. K., Pfister, S. X., Humphrey, T. C., and Strahl, B. D. (2014) Setting the stage for DNA repair. *Nat. Struct. Mol. Biol.* **21,** 655–657
8. Duns, G., van den Berg, E., van Duivenbode, I., Osinga, J., Hollema, H., Hofstra, R. M. W., and Kok, K. (2010) Histone methyltransferase gene *SETD2* is a novel tumor suppressor gene in clear cell renal cell carcinoma. *Cancer Res.* **70,** 4287–4291
9. Dalgliesh, G. L., Furge, K., Greenman, C., Chen, L., Bignell, G., Butler, A., Davies, H., Edkins, S., Hardy, C., Latimer, C., Teague, J., Andrews, J., Barthorpe, S., Beare, D., Buck, G., *et al.* (2010) Inactivation of histone modifiers in RCC. *Nature* **463,** 360–363
10. Grosso, A. R., Leite, A. P., Carvalho, S., Matos, M. R., Martins, F. B., Vítor, A. C., Desterro, J. M., Carmo-Fonseca, M., and de Almeida, S. F. (2015) Pervasive transcription read-through promotes aberrant expression of oncogenes and RNA chimeras in renal carcinoma. *eLife* **4,** e09214
11. Kuo, A. J., Cheung, P., Chen, K., Zee, B. M., Kioi, M., Lauring, J., Xi, Y., Park, B. H., Shi, X., Garcia, B. A., Li, W., and Gozani, O. (2011) NSD2 links dimethylation of histone H3 at lysine 36 to oncogenic programming. *Mol. Cell* **44,** 609–620
12. Lucio-Eterovic, A. K., Singh, M. M., Gardner, J. E., Veerappan, C. S., Rice,

J. C., and Carpenter, P. B. (2010) Role for the nuclear receptor-binding SET domain protein 1 (NSD1) methyltransferase in coordinating lysine 36 methylation at histone 3 with RNA polymerase II function. *Proc. Natl. Acad. Sci. U.S.A.* **107,** 1–6

13. Rosati, R., La Starza, R., Veronese, A., Aventin, A., Schwienbacher, C., Vallespi, T., Negrini, M., Martelli, M. F., and Mecucci, C. (2002) *NUP98* is fused to the *NSD3* gene in acute myeloid leukemia associated with t(8;11)(p11.2;p15). *Blood* **99,** 3857–3860
14. Morishita, M., and di Luccio, E. (2011) Cancers and the NSD family of histone lysine methyltransferases. *BBA - Reviews on Cancer* **1816,** 158–163
15. Stec, I., Wright, T. J., van Ommen, G. J., de Boer, P. A., van Haeringen, A., Moorman, A. F., Altherr, M. R., and den Dunnen, J. T. (1998) *WHSC1*, a 90 kb SET domain-containing gene, expressed in early development and homologous to a *Drosophila* dysmorphy gene maps in the Wolf-Hirschhorn syndrome critical region and is fused to *IgH* in t(4;14) multiple myeloma. *Hum. Mol. Genet.* **7,** 1071–1082
16. Nimura, K., Ura, K., Shiratori, H., Ikawa, M., Okabe, M., Schwartz, R. J., and Kaneda, Y. (2009) NSD2-mediated H3K36me3 links regulate Nkx2–5 to Wolf-Hirschorn syndrome. *Nature* **460,** 287–291
17. Chesi, M., Nardini, E., Lim, R. S., Smith, K. D., Kuehl, W. M., and Bergsagel, P. L. (1998) The t(4;14) translocation in myeloma dysregulates both *FGFR3* and a novel gene, *MMSET*, resulting in IgH/MMSET hybrid transcripts. *Blood* **92,** 3025–3034
18. Keats, J. J., Reiman, T., Maxwell, C. A., Taylor, B. J., Larratt, L. M., Mant, M. J., Belch, A. R., and Pilarski, L. M. (2003) In multiple myeloma, t(4;14)(p16;q32) is an adverse prognostic factor irrespective of FGFR3 expression. *Blood* **101,** 1520–1529
19. Jaffe, J. D., Wang, Y., Chan, H. M., Zhang, J., Huether, R., Kryukov, G. V., Bhang, H.-E. C., Taylor, J. E., Hu, M., Englund, N. P., Yan, F., Wang, Z., McDonald, E. R., Wei, L., Ma, J., *et al.* (2013) *Nat. Genet.* **45,** 1386–1391
20. Oyer, J. A., Huang, X., Zheng, Y., Shim, J., Ezponda, T., Carpenter, Z., Allegretta, M., Okot-Kotber, C. I., Patel, J. P., Melnick, A., Levine, R. L., Ferrando, A., MacKerell, A. D., Jr., Kelleher, N. L., Licht, J. D., and Popovic, R. (2014) Point mutation E1099K in MMSET/NSD2 enhances its methyltranferase activity and leads to altered global chromatin methylation in lymphoid malignancies. *Leukemia* **28,** 198–201
21. Li, F., Mao, G., Tong, D., Huang, J., Gu, L., Yang, W., and Li, G.-M. (2013) The histone mark H3K36me3 regulates human DNA mismatch repair through its interaction with MutSα. *CELL* **153,** 590–600
22. Bua, D. J., Kuo, A. J., Cheung, P., Liu, C. L., Migliori, V., Espejo, A., Casadio, F., Bassi, C., Amati, B., Bedford, M. T., Guccione, E., and Gozani, O. (2009) Epigenome microarray platform for proteome-wide dissection of chromatin-signaling networks. *PLoS ONE* **4,** e6789
23. Dyer, P. N., Edayathumangalam, R. S., White, C. L., Bao, Y., Chakravarthy, S., Muthurajan, U. M., and Luger, K. (2004) Reconstitution of nucleosome core particles from recombinant histones and DNA. *Methods Enzymol.* **375,** 23–44
24. Simon, M. D., Chu, F., Racki, L. R., de la Cruz, C. C., Burlingame, A. L., Panning, B., Narlikar, G. J., and Shokat, K. M. (2007) The site-specific installation of methyl-lysine analogs into recombinant histones. *CELL* **128,** 1003–1012
25. Vermeulen, M., Eberl, H. C., Matarese, F., Marks, H., Denissov, S., Butter, F., Lee, K. K., Olsen, J. V., Hyman, A. A., Stunnenberg, H. G., and Mann, M. (2010) Quantitative interaction proteomics and genome-wide profiling of epigenetic histone marks and their readers. *Cell* **142,** 967–980
26. Moore, K. E., Carlson, S. M., Camp, N. D., Cheung, P., James, R. G., Chua, K. F., Wolf-Yadlin, A., and Gozani, O. (2013) A general molecular affinity strategy for global detection and proteomic analysis of lysine methylation. *Mol. Cell* **50,** 444–456
27. Bartke, T., Vermeulen, M., Xhemalce, B., Robson, S. C., Mann, M., and Kouzarides, T. (2010) Nucleosome-interacting proteins regulated by DNA and histone methylation. *Cell* **143,** 470–484
28. Cox, J., and Mann, M. (2008) MaxQuant enables high peptide identification rates, individualized p.p.b.-range mass accuracies and proteome-wide protein quantification. *Nat Biotechnol* **26,** 1367–1372
29. Méndez, J., and Stillman, B. (2000) Chromatin association of human origin recognition complex, cdc6, and minichromosome maintenance proteins during the cell cycle: assembly of prereplication complexes in late mitosis. *Mol. Cell. Biol.* **20,** 8602–8612
30. Qin, S., and Min, J. (2014) Structure and function of the nucleosome-binding PWWP domain. *Trends Biochem. Sci.* **39,** 536–547
31. Vezzoli, A., Bonadies, N., Allen, M. D., Freund, S. M. V., Santiveri, C. M., Kvinlaug, B. T., Huntly, B. J. P., Göttgens, B., and Bycroft, M. (2010) K36me3 recognition by BRPF1 PWWP. *Nat. Struct. Mol. Biol.* **17,** 617–619
32. van Nuland, R., van Schaik, F. M., Simonis, M., van Heesch, S., Cuppen, E., Boelens, R., Timmers, H. M., and van Ingen, H. (2013) PWWP of PSIP1 binds K36me3 nucleosomes. *Epigenetics Chromatin* **6,** 12
33. Baubec, T., Colombo, D. F., Wirbelauer, C., Schmidt, J., Burger, L., Krebs, A. R., Akalin, A., and Schübeler, D. (2015) DNMT3B PWWP role in genic methylation. *Nature* **520,** 243–247
34. Dhayalan, A., Rajavelu, A., Rathert, P., Tamas, R., Jurkowska, R. Z., Ragozin, S., and Jeltsch, A. (2010) The Dnmt3a PWWP domain reads histone 3 lysine 36 trimethylation and guides DNA methylation. *J. Biol. Chem.* **285,** 26114–26120
35. Li, Y., Trojer, P., Xu, C.-F., Cheung, P., Kuo, A., Drury, W. J., 3rd, Qiao, Q., Neubert, T. A., Xu, R.-M., Gozani, O., and Reinberg, D. (2009) The target of the NSD family of histone lysine methyltransferases depends on the nature of the substrate. *J. Biol. Chem.* **284,** 34283–34295
36. Taverna, S. D., Li, H., Ruthenburg, A. J., Allis, C. D., and Patel, D. J. (2007) How chromatin-binding modules interpret histone modifications: lessons from professional pocket pickers. *Nat. Struct. Mol. Biol.* **14,** 1025–1040
37. Eidahl, J. O., Crowe, B. L., North, J. A., McKee, C. J., Shkriabai, N., Feng, L., Plumb, M., Graham, R. L., Gorelick, R. J., Hess, S., Poirier, M. G., Foster, M. P., and Kvaratskhelia, M. (2013) Structural basis for high-affinity binding of LEDGF PWWP to mononucleosomes. *Nucleic Acids Res.* **41,** 3924–3936
38. Brito, J. L. R., Walker, B., Jenner, M., Dickens, N. J., Brown, N. J. M., Ross, F. M., Avramidou, A., Irving, J. A. E., Gonzalez, D., Davies, F. E., and Morgan, G. J. (2009) MMSET deregulation affects cell cycle progression and adhesion regulons in t(4;14) myeloma plasma cells. *Haematologica* **94,** 78–86
39. Martinez-Garcia, E., Popovic, R., Min, D. J., Sweet, S. M. M., Thomas, P. M., Zamdborg, L., Heffner, A., Will, C., Lamy, L., Staudt, L. M., Levens, D. L., Kelleher, N. L., and Licht, J. D. (2011) The MMSET histone methyl transferase switches global histone methylation and alters gene expression in t(4;14) multiple myeloma cells. *Blood* **117,** 211–220
40. Rosenbloom, K. R., Sloan, C. A., Malladi, V. S., Dreszer, T. R., Learned, K., Kirkup, V. M., Wong, M. C., Maddren, M., Fang, R., Heitner, S. G., Lee, B. T., Barber, G. P., Harte, R. A., Diekhans, M., Long, J. C., *et al.* (2013) ENCODE Data in the UCSC Genome Browser: year 5 update. *Nucleic Acids Res.* **41,** D56-D63
41. Lachner, M., O'Carroll, D., Rea, S., Mechtler, K., and Jenuwein, T. (2001) Methylation of histone H3 lysine 9 creates a binding site for HP1 proteins. *Nature* **410,** 116–120
42. Bannister, A. J., Zegerman, P., Partridge, J. F., Miska, E. A., Thomas, J. O., Allshire, R. C., and Kouzarides, T. (2001) Selective recognition of methylated lyine 9 on histone H3 by the HP1 chromo domain. *Nature* **410,** 120–124
43. Collins, R. E., Northrop, J. P., Horton, J. R., Lee, D. Y., Zhang, X., Stallcup, M. R., and Cheng, X. (2008) The ankyrin repeats of G9a and GLP histone methyltransferases are mono- and dimethyllysine binding modules. *Nat. Struct. Mol. Biol.* **15,** 245–250
44. Margueron, R., Justin, N., Ohno, K., Sharpe, M. L., Son, J., Drury, W. J., 3rd, Voigt, P., Martin, S. R., Taylor, W. R., De Marco, V., Pirrotta, V., Reinberg, D., and Gamblin, S. J. (2009) Role of the polycomb protein EED in the propagation of repressive histone marks. *Nature* **461,** 762–767
45. Lauring, J., Abukhdeir, A. M., Konishi, H., Garay, J. P., Gustin, J. P., Wang, Q., Arceci, R. J., Matsui, W., and Park, B. H. (2008) The multiple myeloma associated MMSET gene contributes to cellular adhesion, clonogenic growth, and tumorigenicity. *Blood* **111,** 856–864